24th INTERNATIONAL CONGRESS ON SOUND AND VIBRATION
23–27 July 2017, London

ICSV24
23-27JULY 2017
LONDON CALLING

A BENCHMARK STRUCTURE FOR VALIDATION OF BLOCKED FORCE TRANSFER PATH ANALYSIS TECHNIQUES

E. A. Pasma, M. V. van der Seijs, D. D. van den Bosch, M. W. F. Wernsen
VIBES.technology, Molengraaffsingel 14, 2629 JD, Delft, The Netherlands
email: epasma@vibestechnology.com

This paper presents a practical study on popular Experimental Dynamic Substructuring topics. A series of substructures is designed of such complexity to fit in right between "real life" structures as often found in industrial applications and "academic" structures which are typically the simplest models to identify a particular phenomenon. The designed benchmark structure comprises an active side with a vibration source, a passive side and a test rig for source characterisation. The connectivity is scalable in complexity, meaning that a single-point, two-point and continuous interface can be established. The vibration source on the active structure is characterised on the test rig using the in-situ TPA concept. Hereafter a component TPA method is applied to simulate the response on the passive side of the coupled structure, in turn obtained by dynamic substructuring. DS-compatible substructure models are obtained from impact measurements using the Virtual Point transformation.

Keywords: transfer path analysis, source characterisation, blocked force

1. Introduction

Dynamic Substructuring (DS), Transfer Path Analysis (TPA) and Source Characterisation (SC) are three research fields that have received tremendous attention from both science and industry. All three aim to provide practical solutions for engineering of structural vibrations and sound, with applications stretching from the automotive and aerospace industry to high-tech precision machinery and sustainable energy solutions. However, it is fair to say that the similarities between the three fields have not always been well understood [1]. This is perhaps motivated by their different origins, for instance: substructuring finds its oldest roots in numerical modelling and reduction of aerospace structures [2–4], transfer path analysis evolved hand-in-hand with automotive NVH engineering [5] and source characterisation emerged from fields such as vibration isolation and structure-borne sound engineering [6, 7]. Only in recent years, some studies [8–10] have appeared that incorporate various aspects of the three fields.

At the same time, many methods within DS, TPA and SC prove to be rather challenging to validate in the context of an industrial application. This is often due to a myriad of experimental uncertainties (signal-to-noise problems, incomparable operational/boundary conditions, presence of secondary excitation sources, etcetera) on top of the applications' inherent complexities. To avoid such uncertainties and reduce the overall complexity of a problem, studies on "academic" structures are often conducted first, such that the method's key properties present themselves as clearly identifiable and unambiguous properties. And although such studies provide an excellent basis for theory development, it remains difficult to transpose a proof of a theoretical concept to application on an industrial problem.

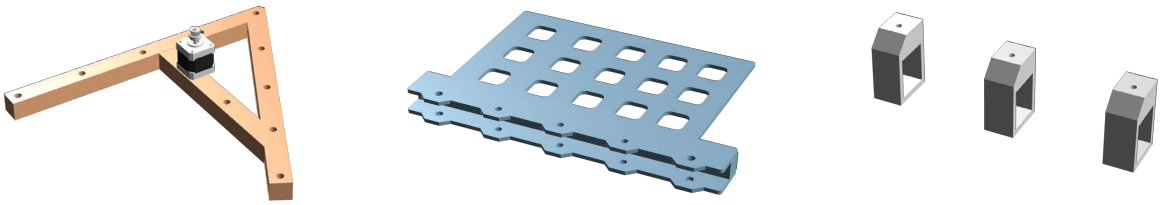

Figure 1: The three benchmark substructures: active source A (left), passive receiver B (centre) and test rig parts R (right).

Paper goal & outline

The goal of this paper is twofold. First, a benchmark structure is proposed of such complexity, that it fits in right between the "real-life" industrial structures on the one hand, and the limited-DoF academic examples on the other hand. Section 2 introduces the three benchmark substructures: an active, passive and test rig substructure. The benchmark substructures have been designed to allow for three different coupling configurations with increasing interface complexity.

The second goal of this paper is to apply concepts of DS, TPA and SC using measurements on the constructed benchmark structures. Section 3 presents a high-level overview of a selection of possible applications, including a virtual point transformation, coupling of substructures A and B, source characterisation of A in test assembly AR and transfer path analysis for prediction of vibrations in assembly AB.

2. Benchmark design

The benchmark construction is motivated by the desire to validate methods within the fields of experimental DS and TPA. More specifically, the aim was to experiment with methods as covered in the general framework articles on the two topics, i.e. [4] and [1]. In the latter one, three types of substructures are used for theory development: an active source structure, a passive receiving structure and a test rig for source characterisation. These substructures form the basis for the benchmark. Also, as the interest is in validating methods in a frequency range of 0 to 5000 Hz, the substructures are supposed to display sufficient dynamics (i.e. vibration modes) in this range.

Figure 1 shows the three substructures. Let us introduce them one by one and briefly touch upon some design considerations:

- Substructure A is welded together from 3 pieces of solid aluminium (30×30 mm). It forms an evenly sided triangle and loosely resembles the character 'A', but was made asymmetric to avoid double resonance modes. It hosts a stepper motor, which is used as the active vibration source. The combined weight is circa 2.5 kg.
- Substructure B is constructed from two plates of stainless steel with a solid piece of steel welded in between. Five holes are placed spanning a total distance of 300 mm, again with 75 mm spacing in between. The total weight is circa 10 kg.
- Substructure R is a collection of small identical support structures, together forming a test rig for testing of substructure A. The test rig R can be used to characterise the source vibrations of substructure A, for prediction of vibrations in an assembly with substructure B. The weight of each support is 670 gramme.

The individual substructures have been designed to allow for various assembly configurations. Figure 2 shows two possible configurations, in this case a single-point connection of substructure A and B and a double-point connection on the test rig.

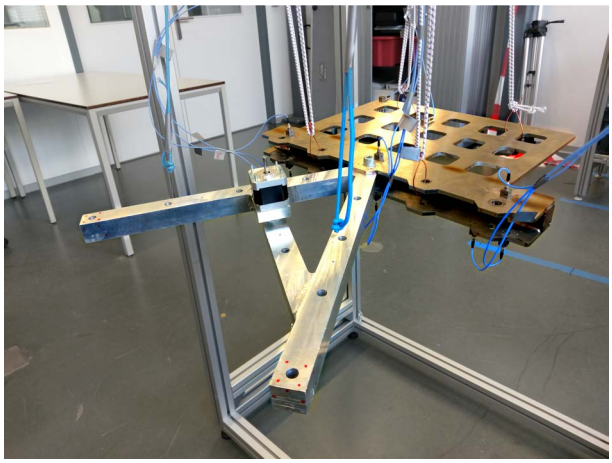

(a) Assembly AB in the single-point coupling configuration, free-floating suspended by soft springs.

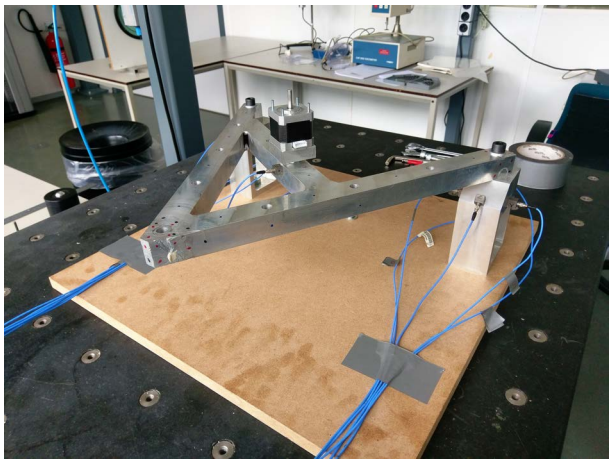

(b) Assembly AR in the two-point coupling configuration, mounted to a wooden base plate.

Figure 2: Two test configurations.

3. Applications

The coming sections provide a high-level overview of some experimental applications, including experimental modelling using virtual point transformation, dynamic substructuring, source characterisation and transfer path analysis.

3.1 Experimental modelling

Experimental modelling can be understood as the art of obtaining a structural-dynamic model (such as FRFs) from measurements [10, 11]. This section briefly discusses how a nodal FRF model can be obtained from impact hammer measurements, demonstrated for experimental modelling of substructures A and B.

3.1.1 Short theory of the Virtual Point Transformation

Typically, experimentally obtained models lack a common interface which allows for substructure coupling. The Virtual Point Transformation [11] introduces such nodes in experimentally obtained models. The main idea is to choose a point on or near a physical interface of a substructure that can be made compatible with the other (experimental or numerical) substructure to couple. All measured displacements $\mathbf{u}$ and forces $\mathbf{f}$ around the interface can be transformed to this virtual point, resulting in a 6-DoF 'nodal' description consisting of virtual translations/rotations $\mathbf{q}$ and forces/moments $\mathbf{m}$:

$$\text{Displacements:} \quad \mathbf{u} = \mathbf{R_u q} \quad \Longrightarrow \quad \mathbf{q} = (\mathbf{R_u})^+ \mathbf{u} \qquad \mathbf{R_u} \in \mathbb{R}^{n\times 6} \tag{1a}$$

$$\text{Forces:} \quad \mathbf{m} = \mathbf{R_f}^T \mathbf{f} \quad \Longrightarrow \quad \mathbf{f} = \left(\mathbf{R_f}^T\right)^+ \mathbf{m} \qquad \mathbf{R_f} \in \mathbb{R}^{m\times 6} \tag{1b}$$

The two transformations allow to compute a 6×6 virtual point FRF matrix $\mathbf{Y_{qm}}(\omega)$ from a measured $n \times m$ matrix $\mathbf{Y}(\omega)$. This can easily be set up for each coupling point, building a experimental 'super-element' that is compatible for substructuring with other models:

$$\text{Measured FRFs:} \quad \mathbf{u} = \mathbf{Y f} \tag{2a}$$

$$\text{Virtual point FRFs:} \quad \mathbf{q} = (\mathbf{R_u})^+ \mathbf{Y} \left(\mathbf{R_f}^T\right)^+ \mathbf{m} \quad \Longrightarrow \quad \mathbf{q} = \mathbf{Y_{qm}} \mathbf{m} \tag{2b}$$

The underlying assumption of this transformation is that the measured substructures behave rigidly in the vicinity of this interface in the frequency range of interest [11].

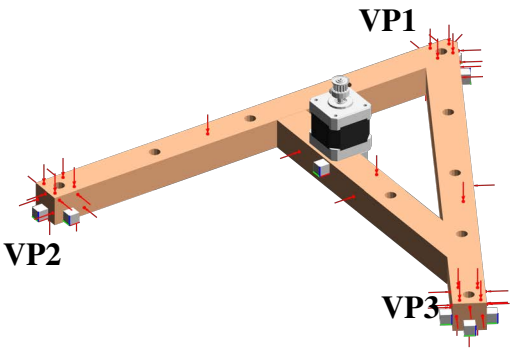

(a) Substructure A. The three coupling points are each instrumented by 3 tri-axial accelerometers and 16 impact points.

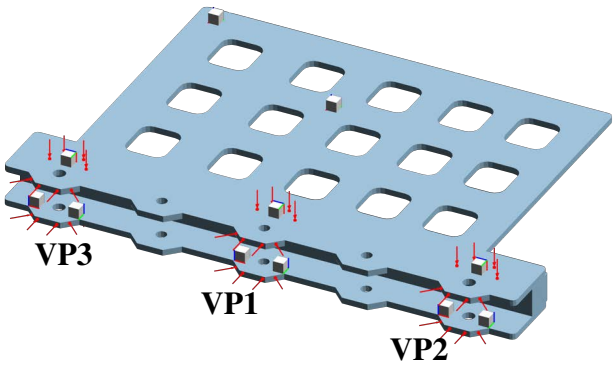

(b) Substructure B. Each coupling point is instrumented by 3 tri-axial accelerometers and 16 impact points; 2 additional sensors register target responses.

Figure 3: Acceleration sensors (indicated by grey cubes) and impact locations (red arrows) visualised on the substructures.

3.1.2 FRF measurement

All substructure FRFs have been obtained by impact hammer testing. Figure 3 depicts how hammer impact points (red arrows) and tri-axial accelerometers (grey cubes) have been positioned and oriented on substructures A and B. Besides some internal points, the main interest for both substructures are the three coupling points. Each coupling point has been instrumented by 3 tri-axial accelerometers of type PCB 356B21. To determine forces and moments, 16 impact hammer positions are chosen per coupling point. Altogether, this results in sufficient overdetermination of the virtual point transformations.

3.1.3 FRF consistency

In order to evaluate the above assumption on rigidity and obtain insight in the contribution of single force impacts or displacements to the VP dynamics, several consistency checks can be done. With a consistency check, the experimentally obtained results are first transformed to the virtual point and then expanded (or projected) back on the original measured DoFs [10, 11]. The difference in the original response and the projected response provides inside on how much residual dynamics (interface flexibility) has been neglected with the virtual point transformation. More practically, this technique is used to evaluate the contribution of single measured DoFs to the transformed VP dynamics. This can be used to find erroneous definitions of sensor and impact positions or directions in the transformation, or discard 'bad impacts'[1] from the transformation.

Let us illustrate the various consistency checks for substructure A. Figure 4a shows the overall sensor consistency of VP2 for excitations around VP1. The score of 100% over the full bandwidth of 5000 Hz indicates that all sensor channels are perfectly consistent, i.e. $\tilde{\mathbf{u}} = \mathbf{u}$. This is obvious as the region between the three sensors is very stiff. Figure 4b shows the overall impact consistency for VP1 with respect to responses around VP2. The light-blue area was computed for all 16 impact points, which is clearly not optimal. Looking into the specific impact consistency for each 16 impacts, three impacts had significant lower score than average. By discarding these 3 from the set of 16, the full 6-DoF set of virtual point forces/moments can still be determined. The dark-blue area was computed for the optimised set, clearly showing an improved overall impact consistency.

[1] Bad impacts can for instance be caused by a low impact energy in the frequency range of interest, low signal-to noise ratio, poor reachability with an impact hammer due to geometric constraints, double pulses, etcetera.

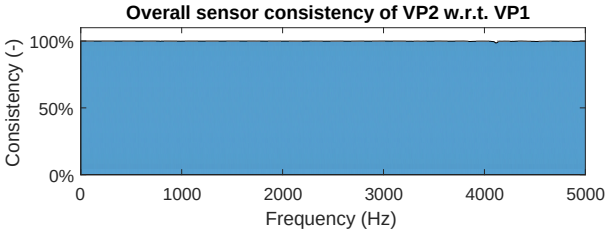

(a) Overall sensor consistency of 9 sensor channels around VP2 with respect to excitations around VP1.

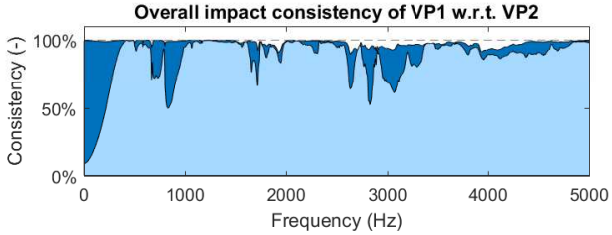

(b) Overall impact consistency of 16 (light blue) and 13 (blue) impacts out of 16 around VP1 with respect to responses around VP2.

Figure 4: Sensor and impact consistency checks for substructure A.

3.2 Dynamic substructuring

Now that VP transformed FRFs are available for substructure A and B, both structures are coupled using the LM-FBS algorithm [4, 12]. To do so, the substructure FRF matrices of A and B are put in block-diagonal form and an appropriate Boolean matrix $\mathbf{B}$ is written (not discussed here):

$$\tilde{\mathbf{Y}} = \mathbf{Y} - \mathbf{Y}\mathbf{B}^T \left(\mathbf{B}\mathbf{Y}\mathbf{B}^T\right)^{-1} \mathbf{B}\mathbf{Y} \qquad \mathbf{Y} \triangleq \begin{bmatrix} \mathbf{Y}^{\mathrm{A}} & \mathbf{0} \\ \mathbf{0} & \mathbf{Y}^{\mathrm{B}} \end{bmatrix} \tag{3}$$

Some results of the substructured FRFs of AB in 2-point coupling configuration are depicted in figure 5. First in 5a, a driving point FRF on the coupling interface is shown, namely for VP2 in Z-direction. The phase is shown as well to assess the passivity[2] of the FRF. Figure 5b shows a transfer FRF from an internal force impact point on structure A to an acceleration response internally on structure B. Both points are not part of a coupling VP, hence the transfer FRF is realised by coupling over the interface. The substructured FRFs (blue) are compared the measured FRFs of the coupled structure AB. It can be seen how resonance frequencies are created at roughly the right frequencies. The phase around anti-resonances is not fully stable, however the overall amplitude of the FRFs match quite well. Note that no filtering or processing has been applied to the measured FRF data, except for transformation to virtual points.

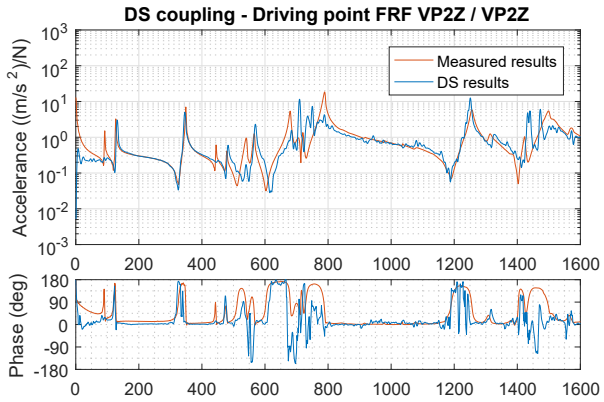

(a) Driving-point FRF for VP3 in Z-direction.

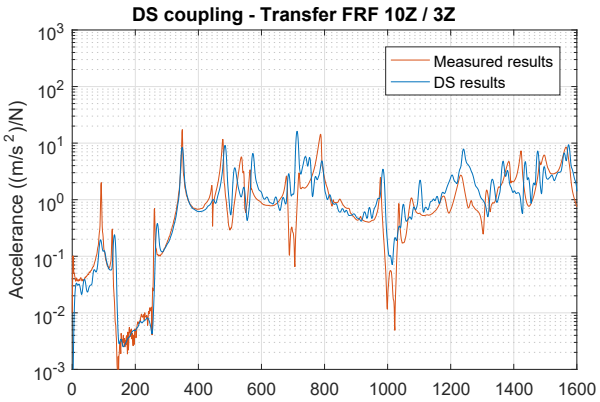

(b) Transfer FRF for an internal impact point on A to an internal response on B, both in Z-direction.

Figure 5: Application of dynamic substructuring: assembled FRFs of AB (blue) in two-point coupling configuration, compared against the validation measurement (red).

[2]For an accelerance driving point FRF, the phase should be bounded by 0 and +180 degrees.

3.3 In-situ source characterisation

To characterise the active vibrations of source structure A, the in-situ characterisation method is used [7]. This method describes the source structure using 'blocked forces' on its interfaces (as if the component were connected to a fully rigid boundary) by measuring operational responses on a connected receiver structure. More specifically, this method is able to characterise a source structure in an assembly, with the resulting characterisation being a property of the source structure only rather than being a property of the combined assembly. Because this characterisation is a source-inherent property, the obtained blocked forces are transferable to other receiving structures. Therefore, in theory, the source may be characterised in the original assembly (e.g. AB) or on a test rig with different dynamic properties (e.g. AR). This paper shows examples of both variants.

The in-situ source characterisation method comprises three steps. Here, it is discussed for the test rig variant; for more explanation of the notation and terminology used, see [1].

1. Operational measurement of the source structure A mounted to a test rig R where indicator responses $\mathbf{u}_4$ on test rig R are measured (see the test setup in figure 2b);
2. FRF measurement of the combined structure AR, more specifically from force inputs at the interface $\mathbf{f}_2$ to the indicator responses on the test rig $\mathbf{u}_4$. Here it is key that the DoFs $\mathbf{u}_4$ are the same set as with the operational measurement;
3. Characterisation of the active source by means of a matrix-inverse operation, resulting in blocked forces for each operational measurement cycle:

$$\mathbf{f}_2^{\text{eq}} = \left(\mathbf{Y}_{42}^{\text{AR}}\right)^{+} \mathbf{u}_4 \tag{4}$$

   where $\mathbf{f}_2^{\text{eq}}$ denotes the blocked forces representing the source structure, $\mathbf{u}_4$ the measured operational responses of step 1 and $\mathbf{Y}_{42}^{\text{AR}}$ the FRFs of the source on test rig measured in step 2.

Note that if a virtual point transformation to a 6-DoF description is done on the force input side of the FRF matrix (i.e. the columns of $\mathbf{Y}_{42}$ relate to forces and moments in virtual point format), the resulting blocked forces $\mathbf{f}_2^{\text{eq}}$ will also present themselves in this form, making them easily transferable to other structures. In other words, one would obtain a source characterisation comprising 3 forces and 3 moments per coupling point, instead of a series of only translational forces.

The source vibrations of the active structure A have been characterised in the original 'target' assembly with passive side B *and* on the test rig structure R. Hence, the two in-situ characterisations yield two sets of 12 blocked forces/moments: 6 for each coupling point. These sets are used for vibration prediction in target assembly AB, which is presented in the next section.

3.4 Component-based Transfer path analysis

For the purpose of virtual noise and vibration prediction , component Transfer Path Analysis is applied on the benchmark data. The advantage of component TPA is the ability to predict target response levels $\mathbf{u}_3$ in/on a passive structure B using an independent source characterisation (i.e. blocked forces) of a source A.

The governing equation of component TPA is as follows:

$$\mathbf{u}_3 = \mathbf{Y}_{32}^{\text{AB}} \mathbf{f}_2^{\text{eq}} \tag{5}$$

where $\mathbf{f}_2^{\text{eq}}$ is a set of equivalent/blocked forces for instance obtained by equation (4) and $\mathbf{Y}_{32}^{\text{AB}}$ the FRF matrix of assembly AB from the interfaces to the responses of interest $\mathbf{u}_3$ (sometimes called Noise Transfer Functions). Combining this with Dynamic Substructuring, one can predict the vibration levels as described above without ever physically assembling structures A and B [9]. In practice, this allows for a separation in development process, since two parties are able to work on their own structures A and B and an interface is provided in terms of blocked forces, possibly in the format of Virtual Point forces and moments.

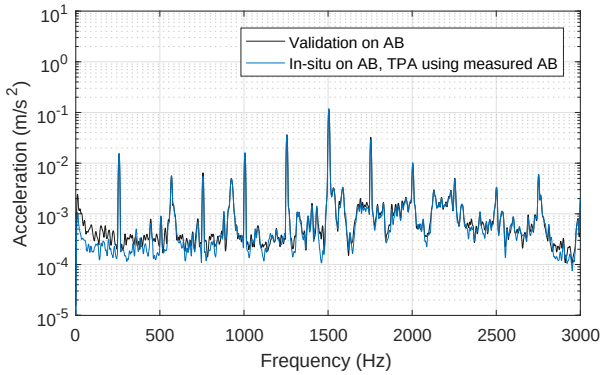

(a) In-situ on AB, TPA prediction using measured FRFs of AB.

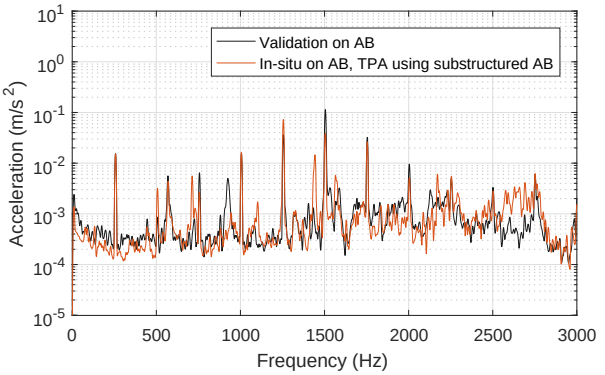

(b) In-situ on AB, TPA prediction using substructured FRFs of AB.

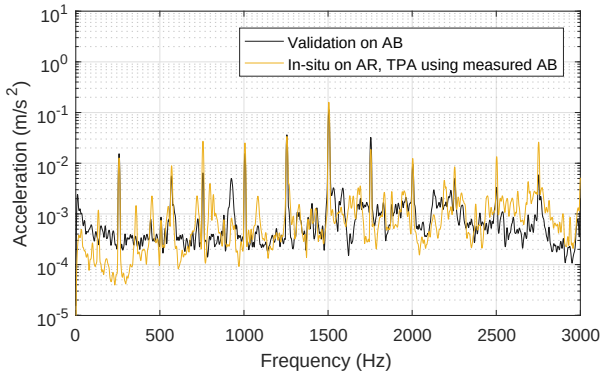

(c) In-situ on AR, TPA prediction using measured FRFs of AB.

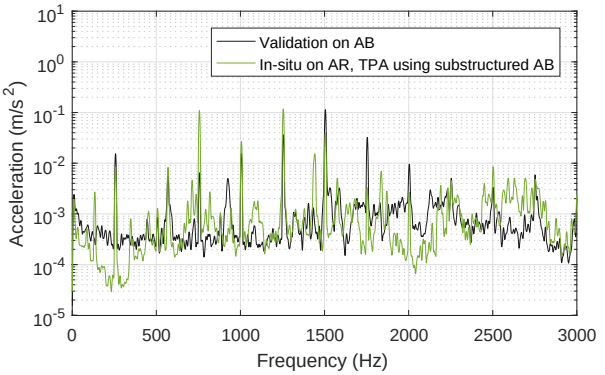

(d) In-situ on AR, TPA prediction using substructured FRFs of AB.

Figure 6: Four results of in-situ source characterisation and TPA prediction (blue/red/yellow/green), all compared to a validation measurement in structure AB (black).

Four results of component TPA are shown in figure 6, namely for source characterisation in AB (top) and AR (bottom) and for component TPA using a measured set of FRFs of AB (left) and substructured FRFs obtained by coupling of A and B (right). A validation response measurement is added for comparison, which is identical for all four plots.

The first result in figure 6a constitutes the most literal application of in-situ TPA: the source is characterised in the original assembly AB, after which the virtual point blocked forces and moments are applied to the same assembly. Near identical results are obtained, especially at the peaks corresponding to the actual signal (source vibration orders) of the stepper motor. Figure 6b shows an application of the same blocked forces to the substructured FRFs of assembly AB. Most peaks are well approximated, which may be considered a very good result considering the various substructure FRF measurements involved (A, B and AB). Note that this approach goes into the direction of virtual vibration prototyping, which heavily relies on the virtual point transformation to provide common interfaces between the various measurements.

The results of figure 6c and 6d present similar results as above, yet for source characterisations calculated from operational measurements on the test rig. The imposed challenge here is that the test rig structure R possesses very different dynamic properties than B, resulting in totally different operational indicator responses ($\mathbf{u}_4^{\mathrm{AR}}$) than in the original assembly ($\mathbf{u}_4^{\mathrm{AB}}$). It is thus interesting to investigate if a source characterisation can be determined that renders similar responses on another passive side, i.e. is *transferable* to arbitrary assemblies. Figure 6c on the left depicts the test rig characterisation applied to the measured FRF of AB. The results are encouraging, as many peaks that exceed the signal noise floor find roughly the right order of magnitude. The noise floor, indeed, has

been a limiting factor in this measurement, as the signal on the test rig sensors hardly exceeded the noise level. Finally, figure 6d shows what might be considered the holy grail of component TPA: a characterisation of source vibrations on a test rig, applied to an experimental model of the target assembly obtained using dynamic substructuring. This indeed constitutes a novelty in experimental DS and TPA, and shall be a direction for further investigation.

4. Conclusions & Outlook

In this paper, a series of benchmark substructures has been presented for method development and validation in the field of DS, TPA and SC. The three benchmark substructures can be connected in several ways, which makes the complexity of the interface problem adjustable to a one-point, two-point or continuous connection. Several applications have been shown to validate methods of experimental modelling, virtual point transformation, dynamic substructuring and source characterisation. Many more validations can be done, which is topic of further research at VIBES.technology.

References

1. van der Seijs, M. V., de Klerk, D. and Rixen, D. J. General framework for transfer path analysis: History, theory and classification of techniques, *Mechanical Systems & Signal Processing*, **68–69**, 217–244, (2016).
2. Hurty, W. C. Vibrations of structural systems by Component Mode Synthesis, *Journal of the Engineering Mechanics Division*, **86** (4), 51–70, (1960).
3. Craig, R. R. J. and Bampton, M. C. C. Coupling of substructures using component mode synthesis, *AIAA Journal*, **6** (7), 1313–1319, (1968).
4. de Klerk, D., Rixen, D. J. and Voormeeren, S. N. General framework for dynamic substructuring: History, review and classifcation of techniques, *AIAA Journal*, **46** (8), 1169–1181, (2008).
5. van der Auweraer, H., Mas, P., Dom, S., Vecchio, A., Janssens, K. and van de Ponseele, P. SAE Technical Paper, Transfer path analysis in the critical path of vehicle refinement: the role of fast, hybrid and operational path analysis, (2007).
6. Mondot, J. M. and Petersson, B. A. T. Characterization of structure-borne sound sources: The source descriptor and the coupling function, *Journal of Sound & Vibration*, **114** (3), 507–518, (1987).
7. Moorhouse, A. T., Elliott, A. S. and Evans, T. A. In situ measurement of the blocked force of structure-borne sound sources, *Journal of Sound & Vibration*, **325** (4–5), 679–685, (2009).
8. de Klerk, D., *Dynamic Response Characterization of Complex Systems through Operational Identification and Dynamic Substructuring*, Ph.D. thesis, Delft University of Technology, The Netherlands, (2009).
9. Rixen, D. J., Boogaard, A., van der Seijs, M. V., van Schothorst, G. and van der Poel, T. Vibration source description in substructuring: A theoretical depiction, *Mechanical Systems & Signal Processing*, **60–61**, 498–511, (2015).
10. van der Seijs, M. V., *Experimental dynamic substructuring: Analysis and design strategies for vehicle development*, Ph.D. thesis, Delft University of Technology, (2016).
11. van der Seijs, M. V., van den Bosch, D. D., Rixen, D. J. and de Klerk, D. An improved methodology for the virtual point transformation of measured frequency response functions in dynamic substructuring, *4th ECCOMAS Thematic Conference on Computational Methods in Structural Dynamics and Earthquake Engineering (COMPDYN)*, Kos Island, Greece, pp. 4334–4347, (2013).
12. de Klerk, D., Rixen, D. and de Jong, J. The frequency based substructuring method reformulated according to the dual domain decomposition method, *Proceedings of the XXIV International Modal Analysis Conference (IMAC), St. Louis, MO*, Bethel, CT, Society for Experimental Mechanics, (2006).